A strategy for designing allosteric modulators of transcription factor dimerization

Sho Oasa, Vladana Vukojević, Rudolf Rigler, Igor Tsigelny, Jean-Pierre Changeux, Lars Terenius

A strategy for designing allosteric modulators of transcription factor dimerization

Sho Oasa[a], Vladana Vukojević[a], Rudolf Rigler[b], Igor F. Tsigelny[c], Jean-Pierre Changeux[d,1], and Lars Terenius[a,1]

[a]Department of Clinical Neuroscience, Karolinska Institutet, SE-17176 Stockholm, Sweden; [b]Department of Medical Biochemistry and Biophysics, Karolinska Institutet, SE-17177 Stockholm, Sweden; [c]Department of Neurosciences, University of California San Diego, La Jolla, CA 92093-0819; and [d]Institut Pasteur, Department of Neuroscience, Unité Neurobiologie Intégrative des Systèmes Cholinergiques, F-75724 Paris 15, France

Contributed by Jean-Pierre Changeux, November 27, 2019 (sent for review September 9, 2019; reviewed by Stuart L. Schreiber and Kurt Wüthrich)

Transcription factors (TFs) are fundamental in the regulation of gene expression in the development and differentiation of cells. They may act as oncogenes and when overexpressed in tumors become plausible targets for the design of antitumor agents. Homodimerization or heterodimerization of TFs are required for DNA binding and the association interface between subunits, for the design of allosteric modulators, appears as a privileged structure for the pharmacophore-based computational strategy. Based on this strategy, a set of compounds were earlier identified as potential suppressors of OLIG2 dimerization and found to inhibit tumor growth in a mouse glioblastoma cell line and in a whole-animal study. To investigate whether the antitumor activity is due to the predicted mechanism of action, we undertook a study of OLIG2 dimerization using fluorescence cross-correlation spectroscopy (FCCS) of live HEK cells transfected with 2 spectrally different OLIG2 clones. The selected compounds showed an effect with potency, which correlated with the earlier observed antitumor activity. The OLIG2 proteins showed change in diffusion time under compound treatment in line with dissociation from DNA. The data suggest a general approach of drug discovery based on the design of allosteric modulators of protein–protein interaction.

transcription factor | OLIG2 | glioblastoma | fluorescence cross-correlation spectroscopy | antitumor agents

The initial work on the bacterial operon (1) and its extension to eukaryotic cell differentiation and embryonic development (2–5) underlined the importance of transcription factors (TFs) as diffusible signaling allosteric proteins, binding to specific DNA elements in the promoter regions and triggering (or inhibiting) in cis the transcription of adjacent genes by DNA–RNA polymerase (6). TFs may, in addition, control the transcription of multiple genes, including their own, thus generating hierarchical trees of gene-expression patterns in the course of development (3, 7, 8). The attempt to extend this paradigm to gene expression in the brain hinges upon the difficulty that hundreds of genetic determinants have been shown to predispose to brain disorders, such as autism-spectrum disorder (ASD) and schizophrenia. Along these lines, analysis of brain gene expression data suggested the concept of coherent-gene groups controlled by TFs (9–11) leading to a strategy to uncover new therapeutic targets for these diseases. Targeting the interfaces of the specific TF dimer-oligomers might interfere with, and even restore, pathological evolution of mutated TFs in genetically predisposed patients.

A first hint about the implementation of the method was the design of new pharmacological agents against glioblastoma. Several studies indicated that the TF, oligodendrocyte lineage transcription factor 2 (OLIG2), is universally expressed in gliomas and is a biomarker for poor prognosis in glioblastomas (12). OLIG2 belongs to a large TF family, bHLH, with a helix–loop–helix DNA binding motif, which first must form homodimers or heterodimers to bind to DNA. Inhibitors which interfere with dimer formation would be ideal antitumor agents. However, the intermolecular surface is shallow and wide, which poses difficulties in generating drug candidates. Computation strategy based on pharmacophore models was introduced to identify potential allosteric dimerization inhibitors. A group of compounds with potential affinity for the intermolecular binding surface was identified (13), and some of the selected compounds were found to inhibit tumor growth in cell culture. However, the molecular mechanisms for the antitumorigenic activity were not experimentally identified. The current study was designed to directly examine the interference with OLIG2 dimerization using fluorescence cross-correlation spectroscopy (FCCS) of 2 spectrally different fluorescent OLIG2 conjugates. FCCS is a powerful technique to quantitatively characterize specific protein–protein interactions in which proteins are labeled by 2 spectrally distinct fluorescent molecules (14). The technique has also been introduced for studies in live cells (15, 16). FCCS provides information of concentrations of unbound and bound molecules, enabling a computation of binding affinity for specific protein–protein interaction in live cells (17). Here, we demonstrate a potential of FCCS to assess compound activity against TF dimerization in live cells.

Results

Effects of Test Compounds on OLIG2 Homodimerization. To assess a direct effect of test compounds on OLIG2 homodimerization, eGFP-fused and Tomato-fused OLIG2, respectively, were transiently coexpressed in HEK cells (*SI Appendix*, Fig. S1*A*). To quantify interaction between OLIG2-eGFP and OLIG2-Tomato, we used FCCS (*SI Appendix*, Fig. S1 *B* and *C*). FCCS enables us to quantify the specific protein–protein interactions to form a

Significance

Transcription factors in the bHLH family are potentially relevant for tumor growth. Activation requires homodimerization or heterodimerization. Thus, the dimerization step is a likely significant drug target. The oligodendrocyte transcription factor 2 (OLIG2) is overexpressed in gliomas. Here, we developed a fluorescence cross-correlation spectroscopy protocol to examine 10 compounds selected using a pharmacophore-based computational strategy targeting OLIG2 dimerization. We showed that the potency to interact with OLIG2 dimerization in live cells correlates with carcinostatic efficacy. The data indicate a promising approach toward drug development targeting transcription factor overactivity and protein–protein interaction more generally.

Author contributions: I.F.T., J.-P.C., and L.T. designed research; S.O. performed research; S.O., V.V., R.R., I.F.T., and J.-P.C. analyzed data; and S.O. and L.T. wrote the paper.

Reviewers: S.L.S., Broad Institute; and K.W., The Scripps Research Institute and ETH Zürich.

The authors declare no competing interest.

[1]To whom correspondence may be addressed. Email: changeux@noos.fr or lars.terenius@ki.se.

This article contains supporting information online at https://www.pnas.org/lookup/suppl/doi:10.1073/pnas.1915531117/-/DCSupplemental.

First published January 17, 2020.

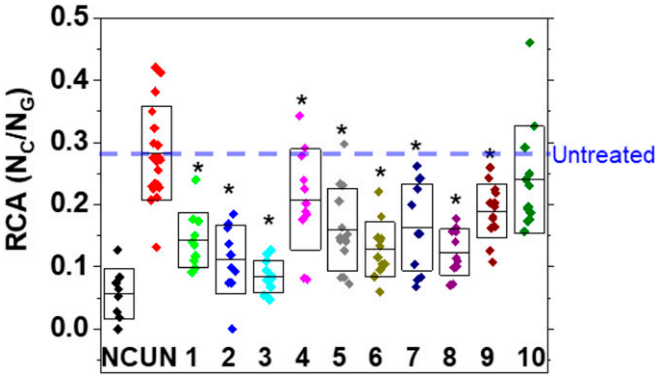

Fig. 1. Inhibitory effect of test compounds on OLIG2 dimerization in live HEK cells. Comparison of RCA in live HEK cells. RCA, N_C/N_G, was calculated from FCCS data. N_C and N_G denote the cross-correlated number and number of OLIG2-eGFP, respectively. Average ± SD in RCA value for negative control (NC) (0.05 ± 0.04), untreated (UN) (0.28 ± 0.07), 1 μM compound #1 (129407: 0.14 ± 0.04), #2 (691240: 0.11 ± 0.06), #3 (50467: 0.08 ± 0.03), #4 (157532: 0.2 ± 0.08), #5 (130815: 0.16 ± 0.06), #6 (219903: 0.13 ± 0.04), #7 (10486: 0.16 ± 0.07), #8 (57144: 0.12 ± 0.04), #9 (13103: 0.19 ± 0.04), #10 (92959: 0.24 ± 0.09). Statistical analysis was performed against untreated (*$P < 0.01$). Blue dashed line shows the average RCA value in untreated cells.

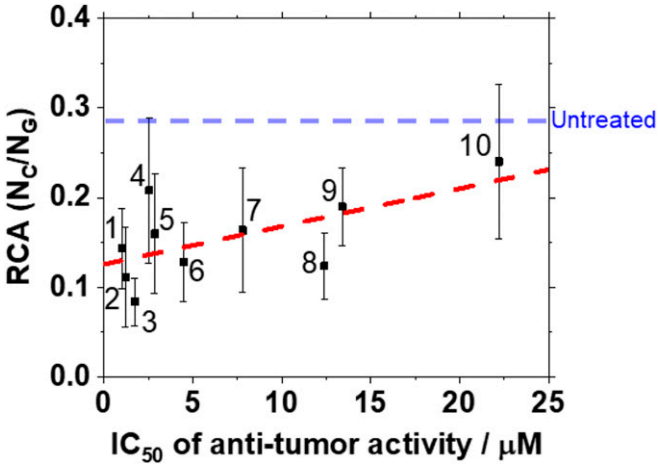

Fig. 2. Correlation analysis of OLIG2 dimerization against IC_{50} tumorigenic cell viability. Linear regression analysis (red dashed line) gave 0.62 Pearson's correlation coefficient based on average values, indicating strong correlation. Blue dashed line shows the average RCA value in untreated cells. Average ± SD in RCA value for negative control (NC) (0.05 ± 0.04), untreated (UN) (0.28 ± 0.07), 1 μM compound #1 (129407: 0.14 ± 0.04), #2 (691240: 0.11 ± 0.06), #3 (50467: 0.08 ± 0.03), #4 (157532: 0.2 ± 0.08), #5 (130815: 0.16 ± 0.06), #6 (219903: 0.13 ± 0.04), #7 (10486: 0.16 ± 0.07), #8 (57144: 0.12 ± 0.04), #9 (13103: 0.19 ± 0.04), #10 (92959: 0.24 ± 0.09). Statistical analysis was performed against untreated.

dimer of two spectrally distinct fluorescent molecules (*SI Appendix*, section 4). To compare the strength of interaction, relative cross-correlation amplitude (RCA) was computed from the number of particles estimated by average autocorrelation and cross-correlation amplitude in individual cells. RCA values of OLIG2 were higher than in a negative control (cells with coexpression of eGFP and Tomato only), indicating OLIG2 dimerization. At 1 μM concentration all test compounds, except for #10 (92959), significantly decreased RCA values (Fig. 1). Strikingly, linear correlation analysis of RCA values against tumorigenic cell viability determined by Tsigelny et al. (13) showed strong correlation (Pearson's correlation coefficient: 0.62) (Fig. 2). Compound #4 (157532) decreased the RCA value significantly but out of linear relationship in Fig. 2. This may suggest that compound #4 (157532) affects tumorigenic cell viability via another inhibitory pathway. To establish test compound concentration dependency, 6 compounds (3 highly effective, 1 intermediate, and 2 less active) were tested. RCA values of all of compounds were decreased in a concentration-dependent manner (Fig. 3 and *SI Appendix*, Fig. S3*A*). Fitting curves to the data, the IC_{50} was determined (*SI Appendix*, Fig. S3*C*). Importantly, RCA values in the presence of 1 μM test compound were strongly correlated with IC_{50} values for OLIG2 homodimerization in live HEK cells (*SI Appendix*, Fig. S3*B*: $R = 0.99$). Therefore, IC_{50} values can be predicted from linear regression line and RCA values (*SI Appendix*, Fig. S3*C*).

Since the OLIG2 homodimer is immobilized by binding to DNA in the cell nucleus, diffusion time analysis was performed by 2-component fitting to separate DNA-bound molecules from molecules in free diffusion (*SI Appendix*, Fig. S2*A* and refs. 18 and 19). The diffusion coefficient in the second component (slow-moving fraction) was not dramatically changed by the treatments (*SI Appendix*, Fig. S2*B*). Compound #5 (130815) gave significantly increased mobility, probably dissociating rapidly from OLIG2 dimer in complex with DNA. In contrast, fractional percentage was significantly and insignificantly decreased against untreated (*SI Appendix*, Fig. S2*C*), suggesting that the DNA-binding fraction decreases by compound treatment, due to OLIG2 dimer dissociation.

Discussion

The field of protein–protein interactions (PPIs) is still a largely uncharted territory for drug design. It has been estimated that the interactome is composed of several hundred thousand PPIs, yet, only a small fraction has still been explored therapeutically.

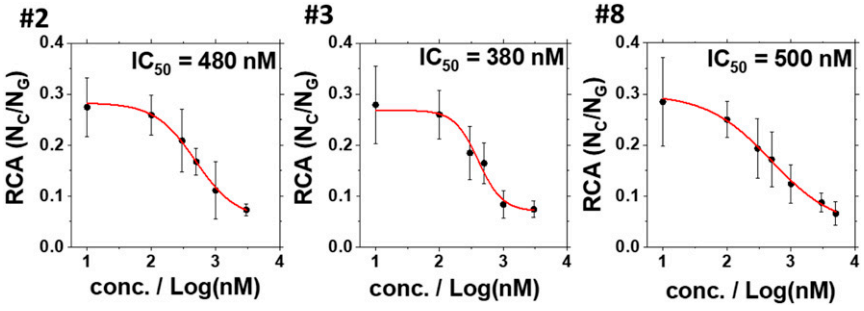

Fig. 3. Dose–response of active compounds. The three most active compounds, which inhibited OLIG2 dimerization effectively were selected for dose–response on dimerization in HEK cells expressing OLIG2-eGFP and OLIG2-Tomato. All compounds showed dose-dependent inhibitory effect for OLIG2 dimerization. Average ± SD in RCA value for #2 (691240) (*Left*), #3 (50467) (*Center*), and #8 (57144) (*Right*). Red solid line denotes curve fitting for determining IC_{50} value in each compound.

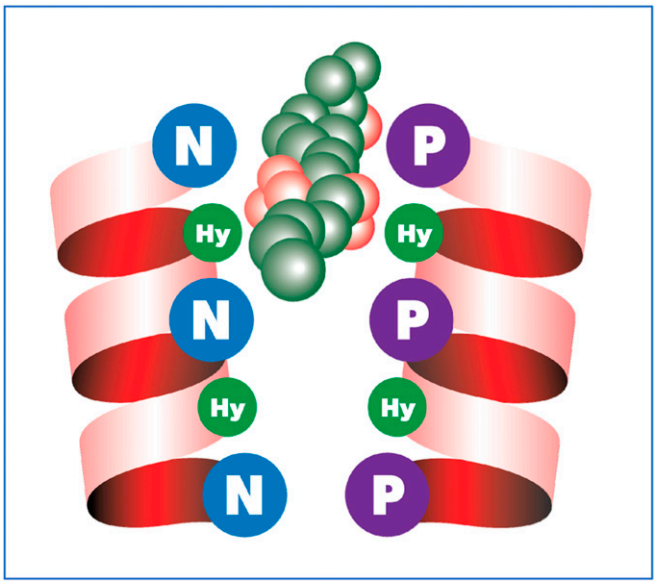

Fig. 4. Schematic diagram of the interaction of a test compound with homodimerization of OLIG2. Hy, hydrophobic site; N, negative charge; P, positive charge.

Studies in silico has defined potential small molecular weight drug candidates (20). Experimentally, in vitro assays are cumbersome since they require significant amounts of pure protein and are not suitable where interactions lead to conformational change in signal transduction (21). Live cell assays with fluorescence-based methodology have been introduced as fluorescence lifetime imaging microscopy (FLIM)-Förster resonance energy transfer (FRET) (22) but FRET is limited to cases where distance between interacting molecules is short and spatially aligned (23). FCCS does not show any of these limitations.

The malignancy of gliomas is a challenge for new drug design. OLIG2 is an obvious target and an intriguing possibility is to introduce inhibition of its dimerization—a crucial step for DNA binding. It is generally known that experimental inhibition of protein–protein interaction is difficult due to commonly wide interaction areas and absence of groves or peaks that give specificity. By molecular modeling it was possible to approximate areas of interaction (in absence of crystal structures) and using computational pharmacophore-based design to predict the compounds that would be possible inhibitors of dimerization leading to antitumor activity. A graphical approach was used in the simulation (Fig. 4). The approach led to selection of molecular candidates, some of which were active in cultures of cells expressing OLIG2. The present data indicate that indeed, cross-correlation analysis revealed inhibition of dimerization. Moreover, the FCCS data correlated with tumor growth inhibition (Fig. 2). The data also suggest that the cross-correlation analysis in live cells could be used to guide development of substances with known mechanism of action in the glioma family of tumors.

Given the medical need, there have been previous attempts to develop inhibition of OLIG2 activity. Peptides "stapled" developed to match the dimer interaction surface were found inactive, possibly due to limited access to the cell interior (24). A recent compound CT-179 has been reported active in a bioassay (25), but its mechanism of action is unclear. In more general terms, the data suggest a general approach of drug discovery based upon the design of allosteric modulators of PPI.

Materials and Methods

Chemicals and Expression Vector Constructs. The selection of test compounds (*SI Appendix*, Fig. S4) was based on in silico modeling with a pharmacophore-based computational strategy. A schematic of the docking of compound 3 (50467) and two OLIG2 molecules is shown in Fig. 4.

The FFT vector constructs were eGFP-fused (OLIG2-eGFP) or Tomato-fused (OLIG2-Tomato). The OLIG2 expression plasmid, pGEM-OLIG2 was kindly provided by Koichi Tabu, Tokyo Medical and Dental University, Tokyo, Japan (26). The OLIG2 region was amplified with PCR using forward primers with XhoI (eGFP) or KpnI (Tomato) restriction sites, and reverse primers with AgeI restriction site using 2× Phusion Master Mix with GC Buffer (Thermo Fisher Scientific). The N1 vectors encoding eGFP or Tomato and PCR-amplified fragments of OLIG2 were digested with XhoI-AgeI or KpnI-AgeI concurrently. The linear N1 vector of eGFP or Tomato and digested OLIG2 fragment were ligated by Instant Sticky-end Ligase Master Mix (NEB).

Cell Culture and Transient Transfection. HEK cells were purchased from ATCC and were maintained in a humidified atmosphere containing 5% CO_2 at 37 °C in Dulbecco's Modified Eagle Medium (Gibco Life Technologies) supplemented with 10% FBS (Gibco), 1% penicillin-streptomycin (Gibco); final concentration 100 U/mL penicillin and 100 μg/mL streptomycin.

One day before the transfection, HEK cells were split into Lab-Tek 8-well Chambered Coverglass (Thermo Fisher Scientific) with 1.0×10^4 (cells/mL in each chamber). HEK cells on an 8-well chamber were transfected with 100 ng of total plasmid DNA (50 ng of OLIG2-eGFP and OLIG2-Tomato; 50 ng of peGFP-N1 and pTomato-N1 as negative controls) and 0.2 μL of Lipofectamine 2000 (Thermo Fisher Scientific). After the transfection, HEK cells were cultured for 24 h. Analysis of a test sample is shown in *SI Appendix*, Fig. S1.

The test compounds were diluted with phenol red free medium, FluoroBrite DMEM (Gibco), for treatment of transfected HEK cells for 1 h at 37 °C. The analysis of a test sample is shown in *SI Appendix*, Fig. S1.

Laser Scanning Microscopy Imaging and Cellular FCCS Measurements. Laser scanning microscopy (LSM) imaging and FCCS measurements were performed using an LSM510 META-ConfoCor3 (Carl Zeiss) equipped with a 488-nm Ar-ion laser, 543 nm He-Ne laser, and a water immersion objective (C-Apochromat, 40×, 1.2 N.A., Corr, Carl Zeiss), and avalanche photodiode detectors (APDs). eGFP and Tomato were excited using the 488-nm laser and 543-nm laser, respectively. The pinhole size was adjusted to 80 μm. The fluorescence of eGFP and Tomato was split by NFT 545. The fluorescence signal of eGFP and Tomato passed through BP505-530 (eGFP) and BP615-680 (Tomato) filter, respectively. FCCS measurements, over the cell nucleus, were carried out 10 times for a duration of 20 s each.

Software and Statistical Analysis. Statistical analysis was performed by 2-sided *t* test on Microsoft Excel. $P < 0.01$ was considered to be statistically significant. Linear regression analysis and dose–response curve fitting were performed using OriginPro 2018. The theoretical curve for fast component of diffusion was drawn by parameters for actual measurement except for fractional percentage of the second component (fraction 2 set to 0) on OriginPro 2018.

Data Availability. Raw data used to generate the figures are available from the corresponding author, L.T., upon request.

ACKNOWLEDGMENTS. We gratefully acknowledge the support of this work by Swedish Research Council Grant VR 2016-01922, an anonymous gift, The Swedish Foundation for Strategic Research Grant SBE13-0115, and The Knut and Alice Wallenberg Foundation Grant KAW 2011.0218 (to L.T.), together with the support of the Human Brain Program SGA2: EU Horizon 2020 Framework Programme Grant No. 785907 (to J.-P.C.). S.O. acknowledges a postdoctoral fellowship from The Nakatani Foundation for Advancement of Measuring Technologies in Biomedical Engineering and a travel grant from Yoshida Foundation for Science and Technology. We thank Dr. Koichi Tabu, Medical Research Institute, Tokyo Medical and Dental University, Tokyo, Japan, for his gift of an OLIG2 expression plasmid. Test compounds were obtained through the National Cancer Institute Chemotherapeutic Agents Repository, Bethesda, MD. The funding agencies had no influence on the study design, methods, data collection, analyses, or the manuscript writing.

1. F. Jacob, J. Monod, Genetic regulatory mechanisms in the synthesis of proteins. *J. Mol. Biol.* **3**, 318–356 (1961).
2. R. J. Britten, E. H. Davidson, Gene regulation for higher cells: A theory. *Science* **165**, 349–357 (1969).
3. E. H. Davidson, Emerging properties of animal gene regulatory networks. *Nature* **468**, 911–920 (2010).
4. W. Driever, C. Nüsslein-Volhard, The bicoid protein is a positive regulator of hunchback transcription in the early Drosophila embryo. *Nature* **337**, 138–143 (1989).

5. J. Jiang, M. Levine, Binding affinities and cooperative interactions with bHLH activators delimit threshold responses to the dorsal gradient morphogen. *Cell* **72**, 741–752 (1993).
6. M. Mannervik, Y. Nibu, H. Zhang, M. Levine, Transcriptional coregulators in development. *Science* **284**, 606–609 (1999).
7. M. Kerszberg, J.-P. Changeux, A simple molecular model of neurulation. *Bioessays* **20**, 758–770 (1998).
8. E. B. Larson *et al*., Striatal regulation of ΔFosB, FosB, and cFos during cocaine self-administration and withdrawal. *J. Neurochem.* **115**, 112–122 (2010).
9. S. Berto, K. Nowick, Species-specific changes in a primate transcription factor network provide insights into the molecular evolution of the primate prefrontal cortex. *Genome Biol. Evol.* **10**, 2023–2036 (2018).
10. O. Hobert, P. Kratsios, Neuronal identity control by terminal selectors in worms, flies, and chordates. *Curr. Opin. Neurobiol.* **56**, 97–105 (2019).
11. I. F. Tsigelny, V. L. Kouznetsova, M. Baitaluk, J.-P. Changeux, A hierarchical coherent-gene-group model for brain development. *Genes Brain Behav.* **12**, 147–165 (2013).
12. P. Y. Wen, S. Kesari, Malignant gliomas in adults. *N. Engl. J. Med.* **359**, 492–507 (2008).
13. I. F. Tsigelny *et al*., Multiple spatially related pharmacophores define small molecule inhibitors of OLIG2 in glioblastoma. *Oncotarget* **8**, 22370–22384 (2017).
14. P. Schwille, F. J. Meyer-Almes, R. Rigler, Dual-color fluorescence cross-correlation spectroscopy for multicomponent diffusional analysis in solution. *Biophys. J.* **72**, 1878–1886 (1997).
15. K. Bacia, S. A. Kim, P. Schwille, Fluorescence cross-correlation spectroscopy in living cells. *Nat. Methods* **3**, 83–89 (2006).
16. N. Szalóki, J. W. Krieger, I. Komáromi, K. Tóth, G. Vámosi, Evidence for homodimerization of the c-fos transcription factor in live cells revealed by fluorescence microscopy and computer modeling. *Mol. Cell. Biol.* **35**, 3785–3798 (2015).
17. M. Tiwari, S. Mikuni, H. Muto, M. Kinjo, Determination of dissociation constant of the NFκB p50/p65 heterodimer using fluorescence cross-correlation spectroscopy in the living cell. *Biochem. Biophys. Res. Commun.* **436**, 430–435 (2013).
18. T. K. Mistri *et al*., Selective influence of Sox2 on POU transcription factor binding in embryonic and neural stem cells. *EMBO Rep.* **16**, 1177–1191 (2015).
19. V. Vukojevic, D. K. Papadopoulos, L. Terenius, W. J. Gehring, R. Rigler, Quantitative study of synthetic Hox transcription factor-DNA interactions in live cells. *Proc. Natl. Acad. Sci. U.S.A.* **107**, 4093–4098 (2010).
20. W.-H. Shin, C. W. Christoffer, D. Kihara, In silico structure-based approaches to discover protein-protein interaction-targeting drugs. *Methods* **131**, 22–32 (2017).
21. J. D. Klemm, S. L. Schreiber, G. R. Crabtree, Dimerization as a regulatory mechanism in signal transduction. *Annu. Rev. Immunol.* **16**, 569–592 (1998).
22. A. Margineanu *et al*., Screening for protein-protein interactions using Förster resonance energy transfer (FRET) and fluorescence lifetime imaging microscopy (FLIM). *Sci. Rep.* **6**, 28186 (2016).
23. A. Illendula *et al*., A small-molecule inhibitor of the aberrant transcription factor CBF -SMMHC delays leukemia in mice. *Science* **347**, 779–784 (2015).
24. A. L. Edwards *et al*., Challenges in targeting a basic helix-loop-helix transcription factor with hydrocarbon-stapled peptides. *ACS Chem. Biol.* **11**, 3146–3153 (2016).
25. G. R. Alton, G. Beaton, S. Knowles, G. Stein, S. Kesari, "Abstract 1174: CT179 degrades the olig2 transcription factor in glioblastoma stem-like cells and prolongs survival" in *Experimental and Molecular Therapeutics* (American Association for Cancer Research, 2017), pp. 1174.
26. K. Tabu *et al*., A novel function of OLIG2 to suppress human glial tumor cell growth via p27Kip1 transactivation. *J. Cell Sci.* **119**, 1433–1441 (2006).